Available online at www.sciencedirect.com
ScienceDirect
Journal of Power Sources 161 (2006) 737–742
JOURNAL OF POWER SOURCES
www.elsevier.com/locate/jpowsour

Manganese oxide film electrodes prepared by electrostatic spray deposition for electrochemical capacitors from the $KMnO_4$ solution

Yang Dai [a,b], Ke Wang [a], Jiachang Zhao [a,b], Jingying Xie [a,b,*]

[a] *Energy Science and Technology Laboratory, Shanghai Institute of Microsystem and Information Technology, Chinese Academy of Sciences, Shanghai 200050, China*
[b] *Graduate School of the Chinese Academy of Science, Beijing 100049, China*

Received 28 February 2006; received in revised form 6 April 2006; accepted 10 April 2006
Available online 12 June 2006

Abstract

Manganese oxide film electrodes for electrochemical capacitors were deposited on the polished Pt foils by electrostatic spray deposition (ESD) from $KMnO_4$ precursor solution. The electrochemical properties of electrodes were systematically studied using cyclic voltammetry (CV), constant current charge–discharge tests, and electrochemical impedance spectroscopy (EIS). The specific capacitance (SC) of thick deposited film was 149 F g^{-1} at the very high scan rate of 500 mV s^{-1}, in comparison with 209 F g^{-1} at the low scan rate of 5 mV s^{-1}. The electrode shows good cyclic performance. The initial SC value was 163 F g^{-1} and 103% of the initial SC can be retained after 10,000 cycles at the scan rate of 50 mV s^{-1}.

Keywords: Electrochemical capacitor; Manganese oxide; Electrostatic spray deposition; Specific capacitance

1. Introduction

Electrochemical capacitors are charge-storage devices of high power and energy density, which exhibit excellent reversibility and a long cycle life. Accordingly, two kinds of electrochemical capacitors have been developed, the electric double layer capacitor and the electrochemical pseudocapacitor. However, carbon electrode of electric double layer capacitor suffers from performance deterioration by oxidation and high internal resistance. Additionally, the mechanism of pseudo-faradic process is not so clear [1,2]. So the electrochemical pseudocapacitor has attracted much attention for its potential application. Among the pseudocapacitor electrode materials, ruthenic oxides and its composite materials have the best electrochemical performances. Their specific capacitance may achieve as high as 700–1000 F g^{-1} [3–6]. However, ruthenic oxides and its composite materials are expensive and toxic to environment. Nowadays, most researches on electrochemical capacitors aim to increase power and energy densities as well as lower fabrication costs while using environmentally friendly materials. So there is increasing interest in the development of electrode materials based on manganese oxides using for electrochemical capacitors [7].

Manganese oxide electrode materials for electrochemical capacitor application have been prepared by various synthetic methods, such as the sol–gel and solution-based chemical routes [4,7–11], electrochemical deposition [1,12–14], and sputtering followed by electrochemical oxidation [15]. Recently, Nam and Kim [16] reported on the synthesis of porous manganese oxide Mn_3O_4 thin film electrodes used in electrochemical capacitors by electrostatic spray deposition (ESD) from $MnCl_2{\cdot}xH_2O$ precursor solution. They suggested that the thin film electrode has an electrochemical oxidation during the cycling process.

In this paper, we reported on the ESD prepared manganese oxide film electrodes from the $KMnO_4$ solution for the electrochemical capacitor. The electrochemical performances were investigated by cyclic voltammetry, constant current charge–discharge tests, and electrochemical impedance spectroscopy. In addition, because the ESD prepared manganese oxide film

* Corresponding author. Tel.: +86 21 62131647; fax: +86 21 32200534.
E-mail address: jyxie@mail.sim.ac.cn (J. Xie).

0378-7753/$ – see front matter © 2006 Elsevier B.V. All rights reserved.
doi:10.1016/j.jpowsour.2006.04.098

electrodes have no binders or conductive additives, it is convenient for us to study the charge-storage mechanism [16].

2. Experimental

2.1. Film deposition

Manganese oxide films were prepared by means of electrostatic spray deposition (ESD) [17]. High dc voltage of 10 kV is applied between an electrically conductive substrate and a needle connecting with a squirm pump. The precursor solution was transported at a proper flow of 3 ml h^{-1} through the squirm pump, and atomized at the tip of the needle 30 mm high above a heated substrate to generate a spray in air atmosphere. The substrate was a thin Pt foil with 1 cm^2 deposited area.

The precursor solution was newly prepared, obtained by dissolving $KMnO_4$ in a mixture of 60 vol.% butyl carbitol, 20 vol.% ethanol and 20 vol.% water. The concentration of $KMnO_4$ in the solution is 0.05 mol l^{-1}. The deposited film electrode was washed with deionized water and dried in air at 60 °C for 10 h. After those processes above, the film is named 'as prepared film'. The mass of the deposit here was in the range of 0.06–0.20 mg cm^{-2}. Unless stated otherwise, the thick film is the mass of 0.12 mg cm^{-2} and deposited at the temperature of 250 °C.

2.2. Characterization

The X-ray diffraction patterns of the electrodes with Pt substrate were detected by means of Rigaku DMAX-2000 diffractometer using a Cu Kα source. The surface morphology of the manganese oxides was observed using a scanning electron microscope (Hitachi S-4700). XPS measurements were performed with PHI 5000C ESCA System (Perkin-Elemer Ltd.).

All the electrochemical measurements were carried out with a Chi-660B potentiostat. The electrochemical measurements were tested by three-electrode electrochemical cell, in which the manganese oxide film electrode was used as the working electrode, Pt plate as the counter and a saturated calomel electrode (SCE) as the reference electrode [16].

Cyclic voltammetry (CV) were performed within a range of 0–0.9 V (versus SCE.) at the scan rates of 5–500 mV s^{-1}. The specific capacitance (SC) was calculated by the following equation:

$$C = \frac{Q}{m\Delta V} \quad (1)$$

The charge (Q) is half of the integrated area of the CV curve; m and ΔV represent the mass of the electrode and the potential window, respectively [18].

Galvanostatic charge–discharge cycling in the potential range of 0–0.9 V was performed at a constant current density of 0.5 mA cm^{-2}. The obtained charge/discharge curves were used for the calculation of SC from the equation below:

$$C = \frac{it}{m\Delta V} \quad (2)$$

where i is the constant discharge current, t the time for discharge, m the total mass of electrode, and ΔV is the voltage change from 0.9 to 0.0 V caused by discharge. Electrochemical impedance measurements were performed in the frequency range of 0.1 Hz to 100 KHz using voltage amplitude of 5 mV before cycling and after 10,000 cycles [18].

3. Results and discussion

3.1. SEM

Even without any binder, the film had good adhesive ability to the substrate. It did not show any abruption even washed for several times and cycled for a long time. Fig. 1 presents the SEM micrographs of ESD prepared manganese oxide film. The film is rough and porous with many cracks. The structure of the ESD prepared manganese oxide is porous, having lots of nano-dimension pores and agglomerates of fine oxide particles. The cracked surface is related to large volume change occurred during the drying process. And it is also partially attributed to

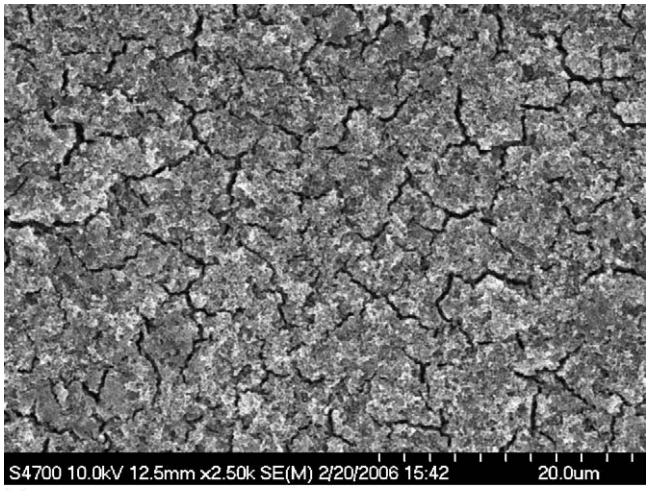

(a)

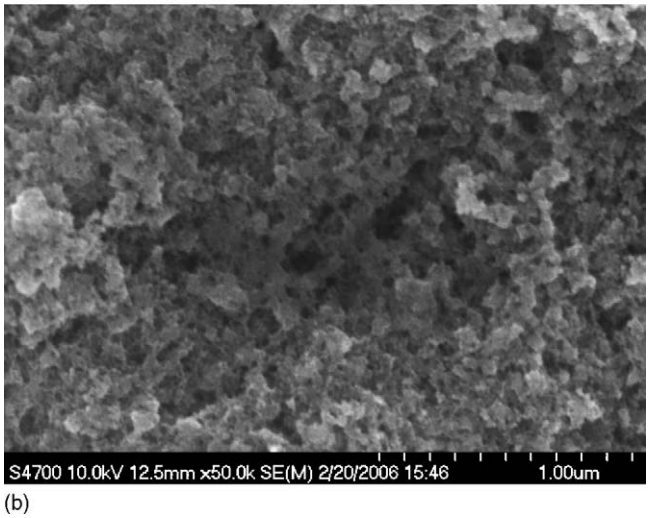

(b)

Fig. 1. SEM pictures for ESD prepared manganese oxide film of 0.12 mg cm^{-2} under a magnification of: (a) 2500 and (b) 50,000.

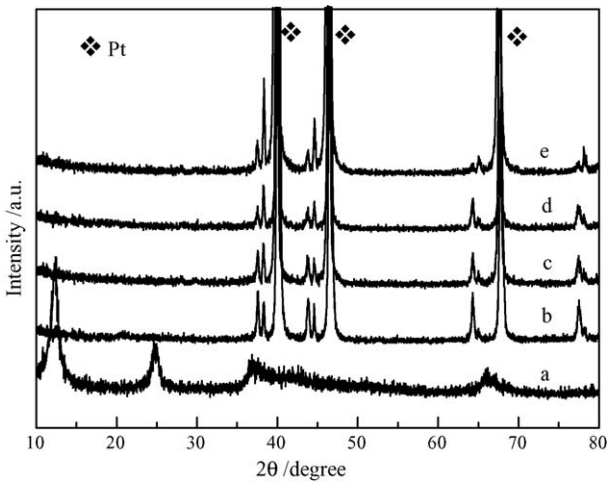

Fig. 2. XRD patterns of: (a) thermal decomposition resultant of $KMnO_4$ at 250 °C in air for 10 h; (b) as prepared film; (c) annealing at 350 °C in air for 10 h; (d) annealing in air at 450 °C for 10 h; (e) after 10,000 CV cycles.

the released gas from the decomposition of $KMnO_4$. The morphology of the manganese oxide film is different from the result of Nam and Kim [16] and other ESD prepared oxide films used in electrochemical capacitor [19,20]. It is probably because the volume change is greater than other precursor solutions during the drying process [21]. The SC value was significantly affected by the surface morphology of the electrode material. The electrolyte was facile to penetrate into the porous and cracked oxide film.

3.2. XRD

Fig. 2 compares the XRD patterns of different manganese oxide film and thermal decomposition resultant of $KMnO_4$. The pattern of as prepared oxide films is unlike that of the decomposition resultant of $KMnO_4$. It is suggested that the resultant of ESD method is different from that of traditional thermal decomposition. However, the pattern is not consistent with any JCPDS cards. Compared with the as prepared film, the patterns of the film after annealing and after 10,000 cycles do not show significant change. The results indicate that the phase of the oxide is very stable even during electrochemical process.

3.3. XPS

Fig. 3(a) presents the typical XPS spectra of the Mn $2p_{3/2}$ orbit of the manganese oxide film electrode. The analytic results indicated that the oxide film was composed of both hydrated trivalent (corresponding to 641.6 eV) and tetravalent (corresponding to 642.6 eV) manganese oxide [1]. And tetravalent manganese oxide was the dominant form. The XPS result indicated that electrochemical irreversible oxide Mn_3O_4 was not detected. It is different from the result of Nam and Kim [16]. Because the initial oxidation state of Mn in $KMnO_4$ was +7, it is reasonable to assume that the oxide film prepared by the thermal decomposition of $KMnO_4$ did not contain Mn^{2+} [22].

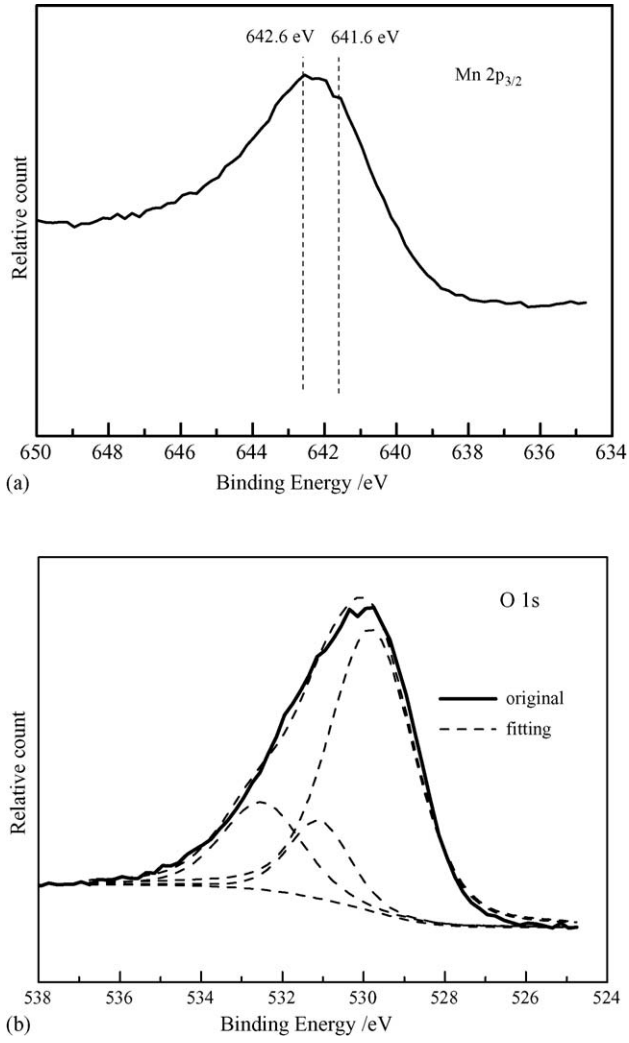

Fig. 3. XPS spectra of: (a) Mn $2p_{3/2}$ and (b) O 1s of the manganese oxide film electrode.

Fig. 3(b) shows the O 1s spectrum of the manganese oxide film electrode. The O 1s spectra were analyzed by curve fitting according to Toupin and co-workers [7]. The spectra can be fitted with three components, which are respectively related to Mn–O–Mn bond (529.8 eV) for the tetravalent oxide, Mn–OH bond (531.1 eV) for a hydrated trivalent oxide, and H–O–H bond (532.5 eV) for residual structure water. The Mn oxidation state is 3.8 calculated from O 1s spectra, which is consistent with the result of the Mn $2p_{3/2}$ spectra. And the fitting peak of 532.5 eV corresponded to the water molecule (H–O–H). The result reveals the oxide is in hydrated form, which is similar to the hydrated form oxide film prepared by electrochemical deposition [1].

3.4. Electrochemical performances

Fig. 4(a) presents CVs of the manganese oxide thick film at the scan rate of 50 mV s^{-1}. The first curve is mostly featureless with the SC of 163 F g^{-1}. With increasing cycle numbers, the voltammetric current decays gradually at the initial cycles but becomes almost constant after 100 cycles. The steady-state

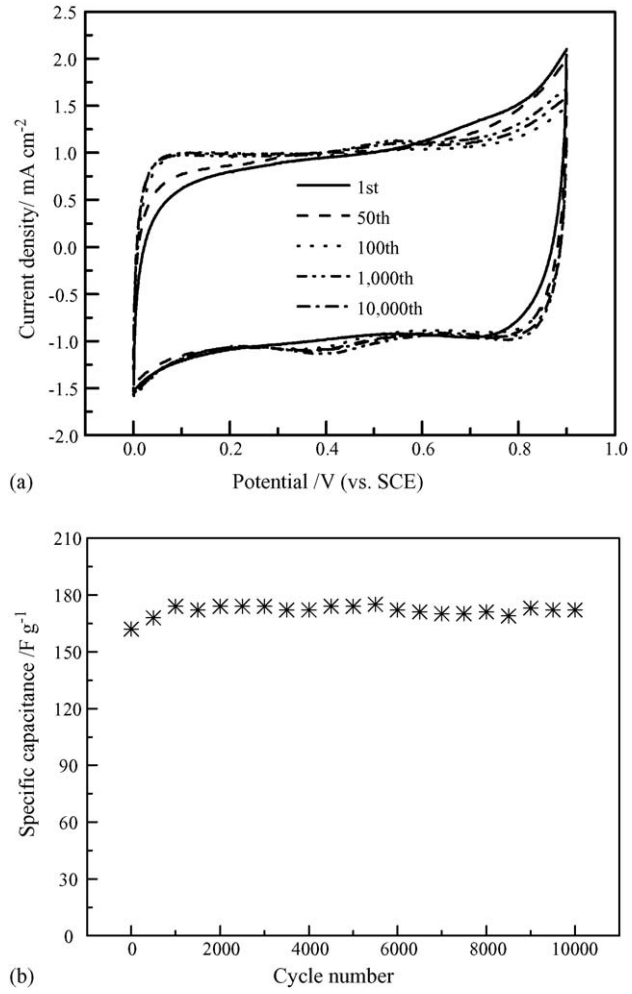

Fig. 4. (a) CVs of different cycles at the scan rate of 50 mV s^{-1} and (b) cycle performance calculated from CVs.

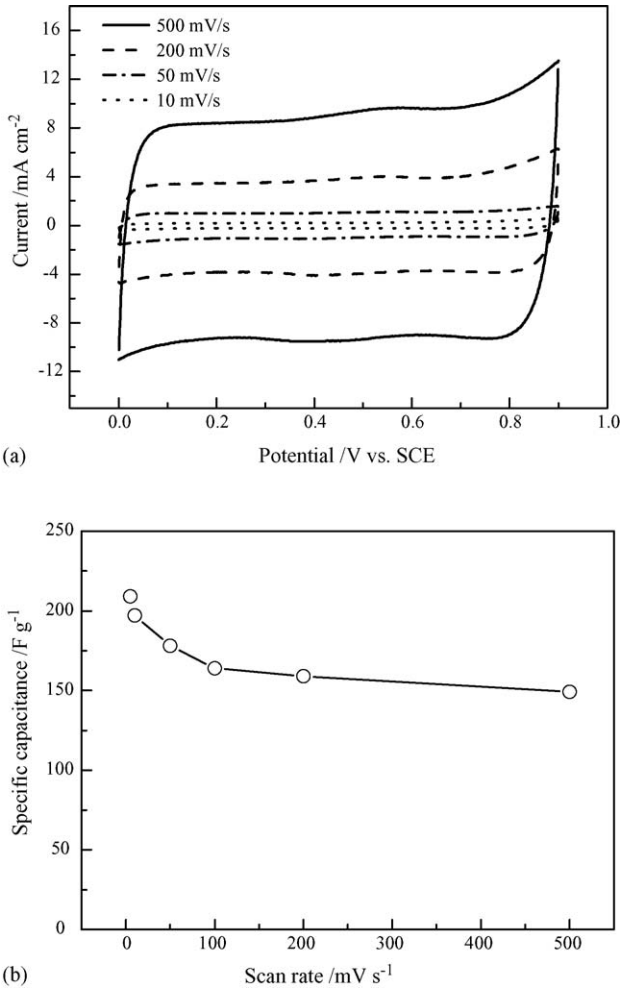

Fig. 5. (a) CVs of different scan rates and (b) effect of different potential scan rate on the specific capacitance of the manganese oxide film electrode.

voltammogram exhibits a rectangular image with broad peaks observed, corresponding to a typical pseudocapacitive behavior where the current flow is independent of the electrode potential [23]. The curves of 100th, 1000th and 10,000th are almost overlapped with the SC of 165, 174 and 172 F g^{-1}, respectively. The broad peaks may be due to redox reactions involving chemisorption or electrosorption of ions on the surface of electrode [24]. Derived from the variation of the shape of CVs, it may undergo a process of electrochemical-activated during the cycling.

Fig. 4(b) shows the cycle performance of the manganese oxide film at the scan rate of 50 mV s^{-1} within the range of 0–0.9 V (versus SCE) in 0.2 M Na_2SO_4 solution. The manganese oxide film shows fairly good cyclic behavior. The maximum SC value 178 F g^{-1} was obtained at the 5000th cycle. The SC value is about 169 F g^{-1} after 10,000 cycles, which is 103% of its initial capacitance. The good cyclic behavior may be ascribed to the phase stabilization of the manganese oxide film (which has been affirmed by the XRD analysis before and after cycling) and the finer adhesion to the substrate. It is notable that the SC value decreased with increasing sample weight. The SC measured at the scan rate of 50 mV s^{-1} was 267, 200 and 135 F g^{-1} corresponding to deposit weights of 0.06, 0.09 and 0.20 mg cm^{-2}, respectively.

Fig. 5(a) presents CVs of different scan rates for the film electrode in the range of 0–0.9 V versus SCE in 0.2 M Na_2SO_4 solution. The shape of all CVs indicated the rectangular and symmetric current–potential characteristics of a capacitor. The CVs are rectangular and symmetrical even at very high scan rate of 500 mV s^{-1}. It indicates excellent electrochemical activity, high reversibility and high power density [25,26].

Fig. 5(b) shows the variation of SC value with the scan rate of CV for the film electrode. The SC values calculated from the CVs were 209, 197, 178, 164 and 159 F g^{-1} for the scan rate of 5, 10, 50, 100 and 200 mV s^{-1}, respectively. Even at the very high rate of 500 mV s^{-1}, SC value 149 F g^{-1} still can be retained, which is 71% of the value obtained at the low scan rate of 5 mV s^{-1}. It reveals the good power character of the film electrode, which may be attributed to the porous and cracked nature of ESD prepared film [16,25].

The charge–discharge behavior of the manganese oxide film was examined by chronopotentiometry [18]. Fig. 6 shows the charge/discharge behavior of the manganese oxide film electrode. The linear and symmetric charge/discharge curves indi-

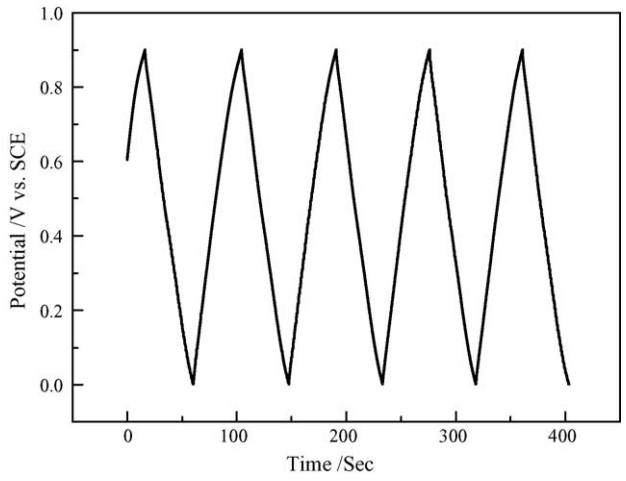

Fig. 6. Charge–discharge curve for the manganese oxide electrode at a constant current density of 0.5 mA cm^{-2}, within a potential range of 0–0.9 V vs. SCE in 0.2 M Na_2SO_4 solution.

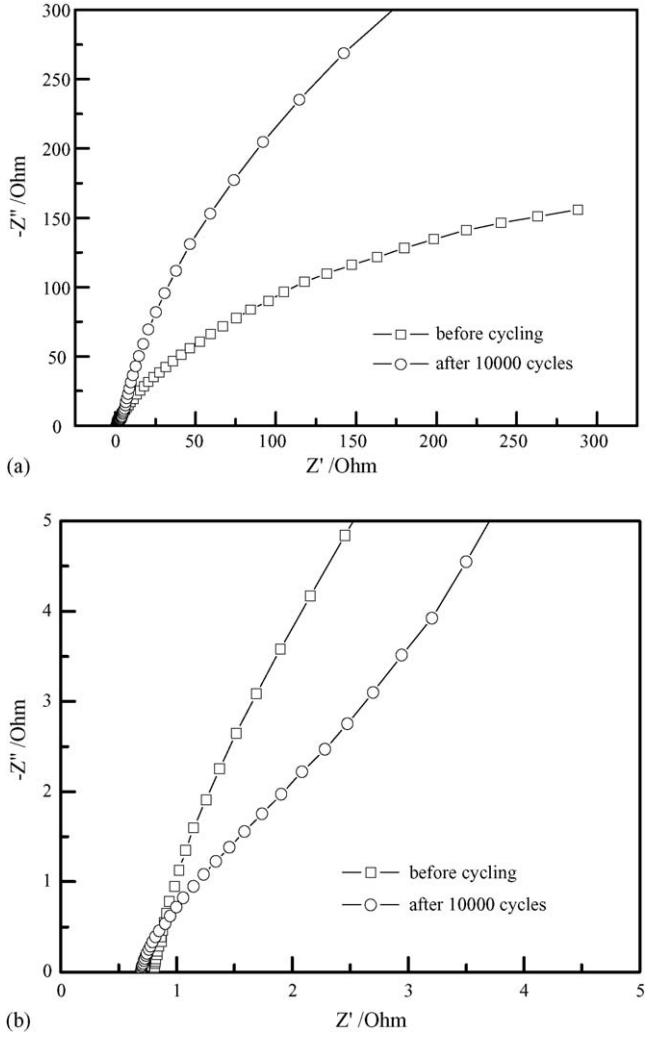

Fig. 7. (a) 0.01–10^6 Hz Nyquist plot for the manganese oxide films before cycling and after 10,000 cycles; (b) high frequency range of the curve.

cate good capacitive and revisable behavior. The SC calculated from the charge/discharge curves according to the Eq. (2) was 207 F g^{-1}, which is close to the SC value of 209 F g^{-1} derived from the CV at the scan rate of 5 mV s^{-1}.

Fig. 7(a) shows the 0.01–10^6 Hz Nyquist plot for the manganese oxide films before and after 10,000 cycles [27]. Both the plots in the high frequency region only show a quarter-distorted circle. For the plot of before cycling, the resistance of electrolyte was about 0.81 Ω cm^{-2} in the high frequency region. In the low-frequency region, the Nyquist diagram shows a slope line, but not so straight. It is interesting that the total resistance 0.69 Ω cm^{-2} of the bulk electrolyte is smaller after 10,000 cycles. And in the low-frequency region, the Nyquist diagram became a 45° slope, which is related to that of the Warbug impedance corresponding to porous nature. This result reveals there is an electrochemical-activated process during the cycling.

4. Conclusion

ESD provides an effective method for preparing film electrodes for electrochemical capacitor. The obtained manganese oxide film from the $KMnO_4$ precursor solution is porous and cracked according to the SEM results. The XRD experiment indicates the phase of the manganese oxide film is stable during the electrochemical process. Analysis of the Mn $2p_{3/2}$ and O 1s XPS spectroscopy revealed that the oxide film prepared at the temperature of 250 °C was mainly in the oxidation state of Mn^{4+} and hydrated form. The thick deposited film of 0.12 mg cm^{-2} was used for electrochemical measurement in 0.2 M Na_2SO_4 solution within the potential range of 0–0.9 V versus SCE. The specific capacitance of thick deposited film was 149 F g^{-1} at the very high scan rate of 500 mV s^{-1}, in comparison with 209 F g^{-1} at the low scan rate of 5 mV s^{-1}. In particular, the film electrode showed fairly good cyclic performance. The initial SC value was 163 F g^{-1} and 103% of the initial SC can be retained after 10,000 cycles at the scan rate of 50 mV s^{-1}. The specific capacitance decreased from 267 to 135 F g^{-1} with increasing loading of the active mass from 0.06 to 0.2 mg cm^{-2}. From the shaped variation of CVs curve and variation of the EIS plots, a process of electrochemical activation is suggested during the cycling. To understand the reaction mechanism better, a further study needs to be done in the near future.

Acknowledgement

The authors gratefully acknowledge Professor Chunhua Chen of USTC for great help in discussion and experiments.

References

[1] J.-K. Chang, W.-T. Tsai, J. Electrochem. Soc. 150 (2003) A1333.
[2] B.E. Conway, Electrochemical Capacitors, Kluwer/Plenum, New York, 1999.
[3] J.P. Zheng, T.R. Jow, J. Electrochem. Soc. 142 (1995) L6.
[4] P. Soudan, J. Gaudet, D. Guay, D. Be langer, R. Schulz, Chem. Mater. 14 (2002) 1210.
[5] W. Sugimoto, H. Iwata, Y. Yasunaga, Y. Murakami, Y. Takasu, Angew. Chem. Int. Ed. 42 (2003) 4092.

[6] I.-H. Kim, J.-H. Kim, Y.-H. Lee, K.-B. Kim, J. Electrochem. Soc. 152 (2005) A2170.
[7] T. Brousse, M. Toupin, D. Bélanger, J. Electrochem. Soc. 151 (2004) A614.
[8] S.C. Pang, M.A. Anderson, T.W. Chapman, J. Electrochem. Soc. 147 (2000) 444.
[9] S.H. Chin, S.C. Pang, M.A. Anderson, J. Electrochem. Soc. 149 (2002) A379.
[10] J.W. Long, A.L. Young, D.R. Rolison, J. Electrochem. Soc. 150 (2003) A1161.
[11] R.N. Reddy, R.G. Reddy, J. Power Sources 124 (2003) 330.
[12] Y.U. Jeong, A. Manthiram, J. Electrochem. Soc. 149 (2002) A1419.
[13] C.C. Hu, T.W. Tsou, Electrochem. Commun. 4 (2002) 105.
[14] C.C. Hu, C.C. Wang, J. Electrochem. Soc. 150 (2003) A1079.
[15] B. Djurfors, J.N. Broughton, M.J. Brett, D.G. Ivey, J. Electrochem. Soc. 153 (2006) A64.
[16] K.-W. Nam, K.-B. Kim, J. Electrochem. Soc. 153 (2006) A81.
[17] C.-Y. Fu, C.-L. Chang, C.-S. Hsu, B.-H. Hwang, Mater. Chem. Phys. 91 (2005) 28.
[18] N. Nagarajan, H. Humadi, I. Zhitomirsky, Electrochim. Acta 51 (15) (2006) 3039–3045.
[19] I.-H. Kim, K.-B. Kim, Electrochem. Solid-State Lett. 4 (2001) A62.
[20] I.-H. Kim, K.-B. Kim, J. Electrochem. Soc. 151 (2004) E7.
[21] A. Princivalle, D. Perednis, R. Neagu, E. Djurado, Chem. Mater. 17 (2005) 1250.
[22] A.-C. Gaillot, D. Flot, V.A. Drits, A. Manceau, M. Burghammer, B. Lanson, Chem. Mater. 15 (2003) 4666.
[23] M. Nakayama, A. Tanaka, Y. Sato, T. Tonosaki, K. Ogura, Langmuir 21 (2005) 5907.
[24] Y. Uk Jeong, Solution-based chemical synthesis of electrode materials for electrochemical power sources, Ph.D. Thesis, The University of Texas at Austin, 2000, pp. 145–150.
[25] K. Rajendra Prasad, N. Miura, Electrochem. Commun. 6 (2004) 1004–1008.
[26] M. Wu, G.A. Snook, G.Z. Chen, D.J. Fray, Electrochem. Commun. 6 (2004) 499.
[27] C. Ye, Z.M. Lin, S.Z. Hui, J. Electrochem. Soc. 152 (2005) A1272.